

Study of inclusive J/psi production in two-photon collisions at LEP II with the DELPHI detector

J. Abdallah, P. Abreu, W. Adam, P. Adzic, T. Albrecht, T. Alderweireld, R. Alemany-Fernandez, T. Allmendinger, P.P. Allport, U. Amaldi, et al.

► **To cite this version:**

J. Abdallah, P. Abreu, W. Adam, P. Adzic, T. Albrecht, et al.. Study of inclusive J/psi production in two-photon collisions at LEP II with the DELPHI detector. Physics Letters B, Elsevier, 2003, 565, pp.76-86. in2p3-00013790

HAL Id: in2p3-00013790

<http://hal.in2p3.fr/in2p3-00013790>

Submitted on 3 Jul 2003

HAL is a multi-disciplinary open access archive for the deposit and dissemination of scientific research documents, whether they are published or not. The documents may come from teaching and research institutions in France or abroad, or from public or private research centers.

L'archive ouverte pluridisciplinaire **HAL**, est destinée au dépôt et à la diffusion de documents scientifiques de niveau recherche, publiés ou non, émanant des établissements d'enseignement et de recherche français ou étrangers, des laboratoires publics ou privés.

Study of Inclusive J/ψ Production in Two-Photon Collisions at LEP II with the DELPHI Detector

DELPHI Collaboration

Abstract

Inclusive J/ψ production in photon-photon collisions has been observed at LEP II beam energies. A clear signal from the reaction $\gamma\gamma \rightarrow J/\psi + X$ is seen. The number of observed $N(J/\psi \rightarrow \mu^+\mu^-)$ events is 36 ± 7 for an integrated luminosity of 617 pb^{-1} yielding a cross-section of $\sigma(J/\psi + X) = 45 \pm 9(\text{stat}) \pm 17(\text{syst}) \text{ pb}$. Based on a study of the event shapes of different types of $\gamma\gamma$ processes in the PYTHIA program, we conclude that $(74 \pm 22)\%$ of the observed J/ψ events are due to ‘resolved’ photons, the dominant contribution of which is most probably due to the gluon content of the photon.

(Accepted by Phys.Lett.B)

J.Abdallah²³, P.Abreu²¹, W.Adam⁴⁸, P.Adzic¹¹, T.Albrecht¹⁶, T.Alderweireld², R.Aleman-Fernandez⁸,
 T.Allmendinger¹⁶, P.P.Allport²², S.Almeida²⁴, U.Amaldi²⁷, N.Amapane⁴³, S.Amato⁴⁵, E.Anashkin³⁴, A.Andreazza²⁶,
 S.Andringa²¹, N.Anjos²¹, P.Antilogus²⁵, W-D.Apel¹⁶, Y.Arnoud¹³, S.Ask²⁴, B.Asman⁴², J.E.Augustin²³,
 A.Augustinus⁸, P.Baillon⁸, A.Ballestrero⁴³, P.Bambade¹⁹, R.Barbier²⁵, D.Bardin¹⁵, G.Barker¹⁶, A.Baroncelli³⁷,
 M.Battaglia⁸, M.Baubillier²³, K-H.Becks⁵⁰, M.Begalli⁶, A.Behrmann⁵⁰, T.Bellunato⁸, N.Benekos³⁰, A.Benvenuti⁵,
 C.Berat¹³, M.Berggren²³, L.Berntzon⁴², D.Bertrand², M.Besancon³⁸, N.Besson³⁸, D.Bloch⁹, M.Blom²⁹, M.Bonesini²⁷,
 M.Boonekamp³⁸, P.S.L.Booth²², G.Borisov^{8,20}, O.Botner⁴⁶, B.Bouquet¹⁹, T.J.V.Bowcock²², I.Boyko¹⁵, M.Bracko⁴¹,
 R.Brenner⁴⁶, E.Brodet³³, P.Bruckman¹⁷, J.M.Brunet⁷, L.Bugge³¹, P.Buschmann⁵⁰, M.Calvi²⁷, T.Camporesi⁸,
 V.Canale³⁶, F.Carena⁸, C.Carimalo²³, N.Castro²¹, F.Cavallo⁵, M.Chapkin⁴⁰, Ph.Charpentier⁸, P.Checchia³⁴,
 R.Chierici⁸, P.Chliapnikov⁴⁰, S.U.Chung⁸, K.Cieslik¹⁷, P.Collins⁸, R.Contri¹², G.Cosme¹⁹, F.Cossutti⁴⁴, M.J.Costa⁴⁷,
 B.Crawley¹, D.Crennell³⁵, J.Cuevas³², J.D'Hondt², J.Dalmau⁴², T.da Silva⁴⁵, W.Da Silva²³, G.Della Ricca⁴⁴,
 A.De Angelis⁴⁴, W.De Boer¹⁶, C.De Clercq², B.De Lotto⁴⁴, N.De Maria⁴³, A.De Min³⁴, L.de Paula⁴⁵, L.Di Ciaccio³⁶,
 A.Di Simone³⁷, K.Doroba⁴⁹, J.Drees⁵⁰, M.Dris³⁰, G.Eigen⁴, T.Ekelof⁴⁶, M.Ellert⁴⁶, M.Elsing⁸, M.C.Espirito Santo⁸,
 G.Fanourakis¹¹, D.Fassouliotis¹¹, M.Feindt¹⁶, J.Fernandez³⁹, A.Ferrer⁴⁷, F.Ferro¹², U.Flagmeyer⁵⁰, H.Foeth⁸,
 E.Fokitis³⁰, F.Fulda-Quenzer¹⁹, J.Fuster⁴⁷, M.Gandelman⁴⁵, C.Garcia⁴⁷, Ph.Gavillet⁸, E.Gazis³⁰, D.Gele⁹, T.Geralis¹¹,
 R.Gokiel^{8,49}, B.Golob⁴¹, G.Gomez-Ceballos³⁹, P.Goncalves²¹, E.Graziani³⁷, G.Grosdidier¹⁹, K.Grzelak⁴⁹, J.Guy³⁵,
 C.Haag¹⁶, F.Hahn⁸, S.Hahn⁵⁰, A.Hallgren⁴⁶, K.Hamacher⁵⁰, K.Hamilton³³, J.Hansen³¹, S.Haug³¹, F.Hauler¹⁶,
 V.Hedberg²⁴, M.Hennecke¹⁶, H.Herr⁸, S-O.Holmgren⁴², P.J.Holt³³, M.A.Houlden²², K.Hultqvist⁴², J.N.Jackson²²,
 Ch.Jarlskog²⁴, G.Jarlskog²⁴, P.Jarry³⁸, D.Jeans³³, E.K.Johansson⁴², P.D.Johansson⁴², P.Jonsson²⁵, C.Joram⁸,
 L.Jungermann¹⁶, F.Kapusta²³, S.Katsanevas²⁵, E.Katsoufis³⁰, R.Keranen¹⁶, G.Kernel⁴¹, B.P.Kersevan^{8,41},
 A.Kiiskinen¹⁴, B.T.King²², N.J.Kjaer⁸, P.Kluit²⁹, P.Kokkinias¹¹, C.Kourkoumelis³, O.Kouznetsov¹⁵, Z.Krumstein¹⁵,
 M.Kucharczyk¹⁷, J.Kurowska⁴⁹, B.Laforge²³, J.Lamsa¹, G.Leder⁴⁸, F.Ledroit¹³, L.Leinonen⁴², R.Leitner²⁸, J.Lemonne²,
 G.Lenzen⁵⁰, V.Lepeltier¹⁹, T.Lesiak¹⁷, W.Liebig⁵⁰, D.Liko^{8,48}, A.Lipniacka⁴², J.H.Lopes⁴⁵, J.M.Lopez³², D.Loukas¹¹,
 P.Lutz³⁸, L.Lyons³³, J.MacNaughton⁴⁸, A.Malek⁵⁰, S.Maltesos³⁰, F.Mandl⁴⁸, J.Marco³⁹, R.Marco³⁹, B.Marechal⁴⁵,
 M.Margoni³⁴, J-C.Marin⁸, C.Mariotti⁸, A.Markou¹¹, C.Martinez-Rivero³⁹, J.Masik²⁸, N.Mastroiannopoulos¹¹,
 F.Matorras³⁹, C.Matteuzzi²⁷, F.Mazzucato³⁴, M.Mazzucato³⁴, R.Mc Nulty²², C.Meroni²⁶, W.T.Meyer¹, E.Migliore⁴³,
 W.Mitaroff⁴⁸, U.Mjoernmark²⁴, T.Moa⁴², M.Moch¹⁶, K.Moenig^{8,10}, R.Monge¹², J.Montenegro²⁹, D.Moraes⁴⁵,
 S.Moreno²¹, P.Morettini¹², U.Mueller⁵⁰, K.Muenich⁵⁰, M.Mulders²⁹, L.Mundim⁶, W.Murray³⁵, B.Muryn¹⁸, G.Myati³³,
 T.Myklebust³¹, M.Nassiakou¹¹, F.Navarria⁵, K.Nawrocki⁴⁹, S.Nemecek²⁸, R.Nicolaidou³⁸, P.Niezurawski⁴⁹,
 M.Nikolenko^{15,9}, A.Nygren²⁴, A.Oblakowska-Mucha¹⁸, V.Obraztsov⁴⁰, A.Olshevski¹⁵, A.Onofre²¹, R.Orava¹⁴,
 K.Osterberg⁸, A.Ouraou³⁸, A.Oyanguren⁴⁷, M.Paganoni²⁷, S.Paiano⁵, J.P.Palacios²², H.Palka¹⁷, Th.D.Papadopoulou³⁰,
 L.Pape⁸, C.Parkes²², F.Parodi¹², U.Parzefall²², A.Passeri³⁷, O.Passon⁵⁰, L.Peralta²¹, V.Perepelitsa⁴⁷, A.Perrotta⁵,
 A.Petrolini¹², J.Piedra³⁹, L.Pieri³⁷, F.Pierre³⁸, M.Pimenta²¹, E.Piotto⁸, T.Podobnik⁴¹, V.Poireau³⁸, M.E.Pol⁶,
 G.Polok¹⁷, P.Poropat⁴⁴, V.Pozdniakov¹⁵, P.Privitera³⁶, N.Pukhaeva^{2,15}, A.Pullia²⁷, J.Rames²⁸, L.Ramler¹⁶, A.Read³¹,
 P.Rebecchi⁸, J.Rehn¹⁶, D.Reid²⁹, R.Reinhardt⁵⁰, P.Renton³³, F.Richard¹⁹, J.Ridky²⁸, I.Ripp-Baudot⁹, D.Rodriguez³⁹,
 A.Romero⁴³, P.Ronchese³⁴, E.Rosenberg¹, P.Roudeau¹⁹, T.Rovelli⁵, V.Ruhlmann-Kleider³⁸, D.Ryabtchikov⁴⁰,
 A.Sadovsky¹⁵, L.Salmi¹⁴, J.Salt⁴⁷, A.Savoy-Navarro²³, C.Schwanda⁴⁸, B.Schwering⁵⁰, U.Schwickerath⁸, A.Segar³³,
 R.Sekulin³⁵, M.Siebel⁵⁰, A.Sisakian¹⁵, G.Smadja²⁵, O.Smirnova²⁴, A.Sokolov⁴⁰, A.Sopczak²⁰, R.Sosnowski⁴⁹,
 T.Spaso⁸, M.Stanitzki¹⁶, A.Stocchi¹⁹, J.Strauss⁴⁸, B.Stugu⁴, M.Szczekowski⁴⁹, M.Szeptycka⁴⁹, T.Szumlak¹⁸,
 T.Tabarelli²⁷, A.C.Taffard²², F.Tegenfeldt⁴⁶, F.Terranova²⁷, J.Timmermans²⁹, N.Tinti⁵, L.Tkatchev¹⁵, M.Tobin²²,
 S.Todorovova⁸, B.Tome²¹, A.Tonazzo²⁷, P.Tortosa⁴⁷, P.Travnicek²⁸, D.Treille⁸, G.Tristram⁷, M.Trochimczuk⁴⁹,
 C.Troncon²⁶, I.A.Tyapkin¹⁵, P.Tyapkin¹⁵, S.Tzamarias¹¹, O.Ullaland⁸, V.Uvarov⁴⁰, G.Valenti⁵, P.Van Dam²⁹,
 J.Van Eldik⁸, A.Van Lysebetten², N.van Remortel², I.Van Vulpen²⁹, G.Vegni²⁶, F.Veloso²¹, W.Venus³⁵, F.Verbeure²,
 P.Verdier²⁵, V.Verzi³⁶, D.Vilanova³⁸, L.Vitale⁴⁴, V.Vrba²⁸, H.Wahlen⁵⁰, A.J.Washbrook²², C.Weiser⁸, D.Wicke⁸,

-
- ¹Department of Physics and Astronomy, Iowa State University, Ames IA 50011-3160, USA
²Physics Department, Universiteit Antwerpen, Universiteitsplein 1, B-2610 Antwerpen, Belgium
and IIHE, ULB-VUB, Pleinlaan 2, B-1050 Brussels, Belgium
and Faculté des Sciences, Univ. de l'Etat Mons, Av. Maistriau 19, B-7000 Mons, Belgium
³Physics Laboratory, University of Athens, Solonos Str. 104, GR-10680 Athens, Greece
⁴Department of Physics, University of Bergen, Allégaten 55, NO-5007 Bergen, Norway
⁵Dipartimento di Fisica, Università di Bologna and INFN, Via Irnerio 46, IT-40126 Bologna, Italy
⁶Centro Brasileiro de Pesquisas Físicas, rua Xavier Sigaud 150, BR-22290 Rio de Janeiro, Brazil
and Depto. de Física, Pont. Univ. Católica, C.P. 38071 BR-22453 Rio de Janeiro, Brazil
and Inst. de Física, Univ. Estadual do Rio de Janeiro, rua São Francisco Xavier 524, Rio de Janeiro, Brazil
⁷Collège de France, Lab. de Physique Corpusculaire, IN2P3-CNRS, FR-75231 Paris Cedex 05, France
⁸CERN, CH-1211 Geneva 23, Switzerland
⁹Institut de Recherches Subatomiques, IN2P3 - CNRS/ULP - BP20, FR-67037 Strasbourg Cedex, France
¹⁰Now at DESY-Zeuthen, Platanenallee 6, D-15735 Zeuthen, Germany
¹¹Institute of Nuclear Physics, N.C.S.R. Demokritos, P.O. Box 60228, GR-15310 Athens, Greece
¹²Dipartimento di Fisica, Università di Genova and INFN, Via Dodecaneso 33, IT-16146 Genova, Italy
¹³Institut des Sciences Nucléaires, IN2P3-CNRS, Université de Grenoble 1, FR-38026 Grenoble Cedex, France
¹⁴Helsinki Institute of Physics, HIP, P.O. Box 9, FI-00014 Helsinki, Finland
¹⁵Joint Institute for Nuclear Research, Dubna, Head Post Office, P.O. Box 79, RU-101 000 Moscow, Russian Federation
¹⁶Institut für Experimentelle Kernphysik, Universität Karlsruhe, Postfach 6980, DE-76128 Karlsruhe, Germany
¹⁷Institute of Nuclear Physics, Ul. Kawioru 26a, PL-30055 Krakow, Poland
¹⁸Faculty of Physics and Nuclear Techniques, University of Mining and Metallurgy, PL-30055 Krakow, Poland
¹⁹Université de Paris-Sud, Lab. de l'Accélérateur Linéaire, IN2P3-CNRS, Bât. 200, FR-91405 Orsay Cedex, France
²⁰School of Physics and Chemistry, University of Lancaster, Lancaster LA1 4YB, UK
²¹LIP, IST, FCUL - Av. Elias Garcia, 14-1^o, PT-1000 Lisboa Codex, Portugal
²²Department of Physics, University of Liverpool, P.O. Box 147, Liverpool L69 3BX, UK
²³LPNHE, IN2P3-CNRS, Univ. Paris VI et VII, Tour 33 (RdC), 4 place Jussieu, FR-75252 Paris Cedex 05, France
²⁴Department of Physics, University of Lund, Sölvegatan 14, SE-223 63 Lund, Sweden
²⁵Université Claude Bernard de Lyon, IPNL, IN2P3-CNRS, FR-69622 Villeurbanne Cedex, France
²⁶Dipartimento di Fisica, Università di Milano and INFN-MILANO, Via Celoria 16, IT-20133 Milan, Italy
²⁷Dipartimento di Fisica, Univ. di Milano-Bicocca and INFN-MILANO, Piazza della Scienza 2, IT-20126 Milan, Italy
²⁸IPNP of MFF, Charles Univ., Areal MFF, V Holesovickach 2, CZ-180 00, Praha 8, Czech Republic
²⁹NIKHEF, Postbus 41882, NL-1009 DB Amsterdam, The Netherlands
³⁰National Technical University, Physics Department, Zografou Campus, GR-15773 Athens, Greece
³¹Physics Department, University of Oslo, Blindern, NO-0316 Oslo, Norway
³²Dpto. Física, Univ. Oviedo, Avda. Calvo Sotelo s/n, ES-33007 Oviedo, Spain
³³Department of Physics, University of Oxford, Keble Road, Oxford OX1 3RH, UK
³⁴Dipartimento di Fisica, Università di Padova and INFN, Via Marzolo 8, IT-35131 Padua, Italy
³⁵Rutherford Appleton Laboratory, Chilton, Didcot OX11 0QX, UK
³⁶Dipartimento di Fisica, Università di Roma II and INFN, Tor Vergata, IT-00173 Rome, Italy
³⁷Dipartimento di Fisica, Università di Roma III and INFN, Via della Vasca Navale 84, IT-00146 Rome, Italy
³⁸DAPNIA/Service de Physique des Particules, CEA-Saclay, FR-91191 Gif-sur-Yvette Cedex, France
³⁹Instituto de Física de Cantabria (CSIC-UC), Avda. los Castros s/n, ES-39006 Santander, Spain
⁴⁰Inst. for High Energy Physics, Serpukov P.O. Box 35, Protvino, (Moscow Region), Russian Federation
⁴¹J. Stefan Institute, Jamova 39, SI-1000 Ljubljana, Slovenia and Laboratory for Astroparticle Physics,
Nova Gorica Polytechnic, Kostanjevska 16a, SI-5000 Nova Gorica, Slovenia,
and Department of Physics, University of Ljubljana, SI-1000 Ljubljana, Slovenia
⁴²Fysikum, Stockholm University, Box 6730, SE-113 85 Stockholm, Sweden
⁴³Dipartimento di Fisica Sperimentale, Università di Torino and INFN, Via P. Giuria 1, IT-10125 Turin, Italy
⁴⁴Dipartimento di Fisica, Università di Trieste and INFN, Via A. Valerio 2, IT-34127 Trieste, Italy
and Istituto di Fisica, Università di Udine, IT-33100 Udine, Italy
⁴⁵Univ. Federal do Rio de Janeiro, C.P. 68528 Cidade Univ., Ilha do Fundão BR-21945-970 Rio de Janeiro, Brazil
⁴⁶Department of Radiation Sciences, University of Uppsala, P.O. Box 535, SE-751 21 Uppsala, Sweden
⁴⁷IFIC, Valencia-CSIC, and D.F.A.M.N., U. de Valencia, Avda. Dr. Moliner 50, ES-46100 Burjassot (Valencia), Spain
⁴⁸Institut für Hochenergiephysik, Österr. Akad. d. Wissensch., Nikolsdorfergasse 18, AT-1050 Vienna, Austria
⁴⁹Inst. Nuclear Studies and University of Warsaw, Ul. Hoza 69, PL-00681 Warsaw, Poland
⁵⁰Fachbereich Physik, University of Wuppertal, Postfach 100 127, DE-42097 Wuppertal, Germany

1 Introduction

An important component of the e^+e^- collisions at LEP II energy is the two-photon fusion process. It has been pointed out that two-photon production of inclusive J/ψ mesons:

$$e^+ + e^- \rightarrow e^+ + e^- + \gamma_1 + \gamma_2, \quad (1)$$

$$\gamma_1 + \gamma_2 \rightarrow J/\psi + X. \quad (2)$$

is a sensitive channel for investigating the gluon distribution in the photon [1].

There are two important processes leading to inclusive J/ψ production. The corresponding typical diagrams are given in Fig. 1a–b. Less important diagrams are not considered here. The first process is described by the vector-meson dominance (VDM) model [2]:

$$\gamma_1 \rightarrow c + \bar{c}, \quad \gamma_2 \rightarrow q + \bar{q} \quad \text{and} \quad \gamma_1 + \gamma_2 \rightarrow J/\psi + q + \bar{q}, \quad (3)$$

as shown in Fig. 1a. The vertices for γ_1 and γ_2 are connected by Pomeron exchange or diffractive dissociation of photons. The final-state parton pairs $c + \bar{c}$ and $q + \bar{q}$ are both in the state of $J^{PC} = 1^{--}$, which means that the latter is dominated by the low-mass vector mesons ρ^0 , ω and ϕ but a more general inclusive hadronization of the partons may also be important.

The second process is described, for example, by the colour-octet model [3]. It proceeds through the so-called ‘resolved’ contribution of the photons, in which the intermediate photons are ‘resolved’ into their constituent partons:

$$\gamma_1 + g_\gamma \rightarrow c + \bar{c}, \quad \gamma_2 + g_\gamma \rightarrow q + \bar{q}, \quad \text{and} \quad \gamma_1 + \gamma_2 \rightarrow J/\psi + q + \bar{q}, \quad (4)$$

as shown in Fig. 1b.

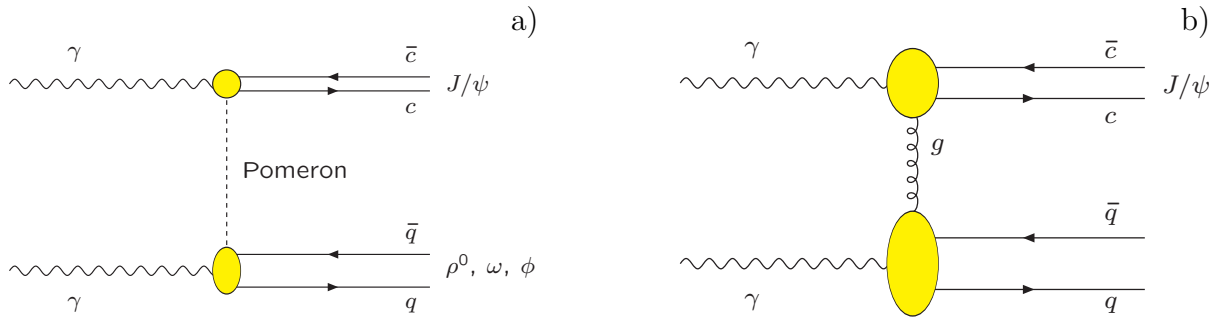


Figure 1: Inclusive J/ψ production in $\gamma\gamma$ processes: a) through vector-meson dominance, b) via gluon content of the photon, i.e. ‘resolved’ contributions.

It is seen that this process requires production of a ‘resolved’ gluon (g_γ) from both photons. Thus, this production mechanism provides a sensitive probe of the gluon content of the photon.

The purpose of this letter is to report the observation of inclusive J/ψ production from the two-photon fusion process, to give its production characteristics along with the cross-section and finally to assess the relative importance of the production processes discussed above. Section 2 describes the selection criteria for the event sample collected for this study. The measurement of inclusive J/ψ production in the $\mu^+\mu^-$ channel and its interpretation in terms of diffractive and resolved processes is presented in section 3 followed by a summary and conclusions.

2 Experimental Procedure

The analysis presented here is based on the data taken with the DELPHI detector [4,5] during the years 1996–2000, excluding the part of the data collected in the last period of 2000, when one of the Time Projection Chamber (TPC) sectors was not in operation. The centre-of-mass energies \sqrt{s} for LEP ranged from 161 to 207 GeV. The total integrated luminosity used in the analysis is 617 pb^{-1} .

The charged particle tracks were measured in the 1.2 T magnetic field by a set of tracking detectors including the microVertex Detector (VD), the Inner Detector (ID), the TPC, the Outer Detector (OD) and the Forward/Backward Chambers FCA and FCB. The following selection criteria were applied:

- (a) particle momentum $p > 200 \text{ MeV}/c$;
- (b) relative momentum error of a track $\Delta p/p < 100\%$;
- (c) impact parameter of a track, transverse to the beam axis $< 3 \text{ cm}$;
- (d) impact parameter of a track, along the beam axis $< 7 \text{ cm}$;
- (e) polar angle of a track, with respect to the beam axis $10^\circ < \theta < 170^\circ$;
- (f) track length $> 30 \text{ cm}$.

The neutral particles (γ , π^0 , K_L^0 , n) were selected by demanding that the calorimetric information, not associated with charged particle tracks, satisfies the following cuts:

- (g) $E(\text{neutral}) > 0.2 \text{ GeV}$ for the electromagnetic showers, unambiguously identified as photons;
- (h) $E(\text{neutral}) > 0.5 \text{ GeV}$ for all the other showers;
- (i) polar angle of neutral particle tracks, with respect to the beam axis $10^\circ < \theta < 170^\circ$.

In order to ensure a very high trigger efficiency, the selected events were required to satisfy at least *one* of the following sets of criteria:

- (j₁) one or more charged particle tracks in the barrel region ($40^\circ < \theta < 140^\circ$) with $p_t > 1.2 \text{ GeV}/c$, is found;
- (j₂) one or more neutral particle tracks in the Forward ElectroMagnetic Calorimeter (FEMC) ($10^\circ < \theta < 36^\circ$ and $144^\circ < \theta < 170^\circ$) with energy greater than 10 GeV, is found;
- (j₃) the total sum of charged particle tracks in the barrel with $p_t > 1 \text{ GeV}/c$, of charged particle tracks in the forward region ($10^\circ < \theta < 40^\circ$ or $140^\circ < \theta < 170^\circ$) with $p_t > 2 \text{ GeV}/c$ and of neutral particle tracks in the FEMC with $E > 7 \text{ GeV}$, is greater than one;
- (j₄) the total sum of charged particle tracks in the barrel with $p_t > 0.5 \text{ GeV}/c$, of charged particle tracks in the forward region with $p_t > 1 \text{ GeV}/c$ and of neutral particle tracks in the FEMC with $E > 5 \text{ GeV}$, is greater than four.

The trigger efficiency for the events which passed the above requirements is bigger than 98%.

The hadronic two-photon events are characterized by a low visible invariant mass. Consequently, the following additional cuts were applied:

- (k) the visible invariant mass, W_{vis} , calculated from the four-momentum vectors of the measured charged and neutral particle tracks, is less than $35 \text{ GeV}/c^2$;
- (l) the number of charged particle tracks N_{ch} satisfies $4 \leq N_{\text{ch}} \leq 30$;
- (m) the sum of the transverse energy components with respect to the beam direction for all charged particle tracks ($\sum \sqrt{p_t^2 + m_\pi^2}$) is greater than 3 GeV.

The comparison of the W_{vis} distributions, after the cuts on N_{ch} and $\sum E_T^{\text{vis}}$, both for the data and the events simulated by PYTHIA, shows (Fig. 2) that the cut $W_{\text{vis}} \leq 35 \text{ GeV}/c^2$ rejects the major part of the non-two-photon events.

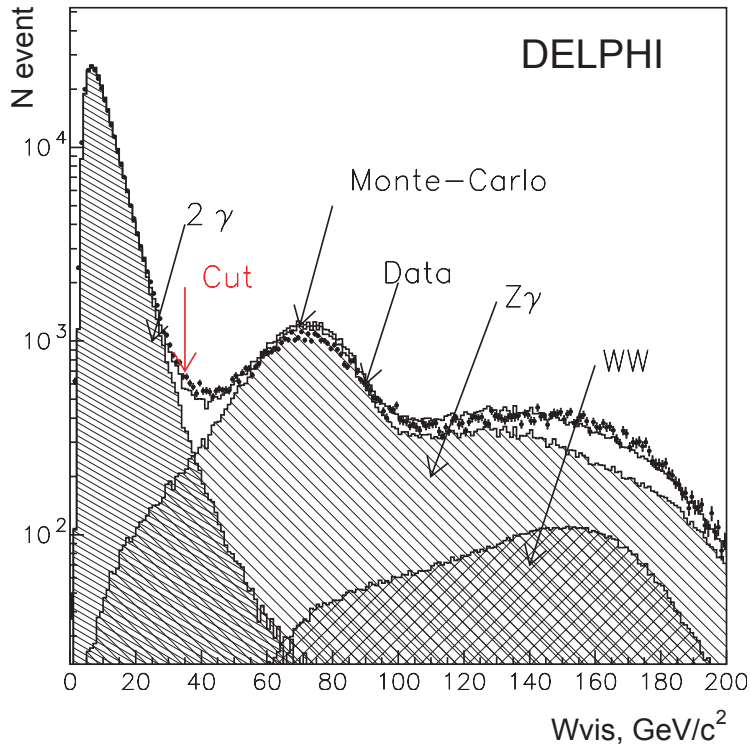


Figure 2: W_{vis} distributions for the LEP II DELPHI data, for the simulated $\gamma\gamma \rightarrow \text{hadrons}$, $e^+e^- \rightarrow Z^0\gamma$, $e^+e^- \rightarrow W^+W^-$ and the sum of all above Monte-Carlo contributions

A total of $N_t = 274\,510$ events remain in the data sample after applying all these cuts. The main background comes from the process $e^+e^- \rightarrow Z\gamma$ and amounts to $\sim 1.2\%$ of the selected $\gamma\gamma$ events. The background from the $e^+e^- \rightarrow W^+W^-$ is negligible, as seen in Fig. 2.

J/ψ candidates have been selected using the $\mu^+\mu^-$ decay channel. For the muon pair selection, the following criteria were imposed:

- (n) at least two charged particle tracks, with zero net charge, should be accepted by the standard DELPHI muon-tagging algorithm [5], or be identified as muons by the hadronic calorimeter;
- (o) the tracks should not come from any reconstructed secondary vertex or be identified as a kaon, proton or electron by the standard DELPHI identification packages.

3 Inclusive J/ψ Production

In this section, we first determine the inclusive J/ψ production in the $\mu^+\mu^-$ channel. Then we interpret it in terms of diffractive and resolved processes by fitting the experimental $p_T^2(J/\psi)$ distribution to the PYTHIA predictions for both processes. This allows to deduce the cross-section for inclusive J/ψ production, taking into account the

$\gamma\gamma \rightarrow J/\psi + X$ and the $J/\psi \rightarrow \mu^+\mu^-$ efficiencies. As the first set of efficiencies is model-dependent, we also give the ‘visible’ cross-section in which only the detector efficiency for $J/\psi \rightarrow \mu^+\mu^-$ decay is considered. We finally present the J/ψ production characteristics together with the PYTHIA predictions.

In Fig. 3 we give the invariant mass distribution for identified $\mu^+\mu^-$ pairs, selected as outlined in the previous section. The J/ψ signal shows up over little background. A least squares fit to the $M(\mu^+\mu^-)$ distribution with a Gaussian for the signal and a second order polynomial for the background gives the following results:

$$\begin{aligned} J/\psi \text{ mass: } M &= 3119 \pm 8 \text{ MeV}/c^2, \\ J/\psi \text{ width: } \sigma(\text{obs}) &= 35 \pm 7 \text{ MeV}/c^2. \end{aligned}$$

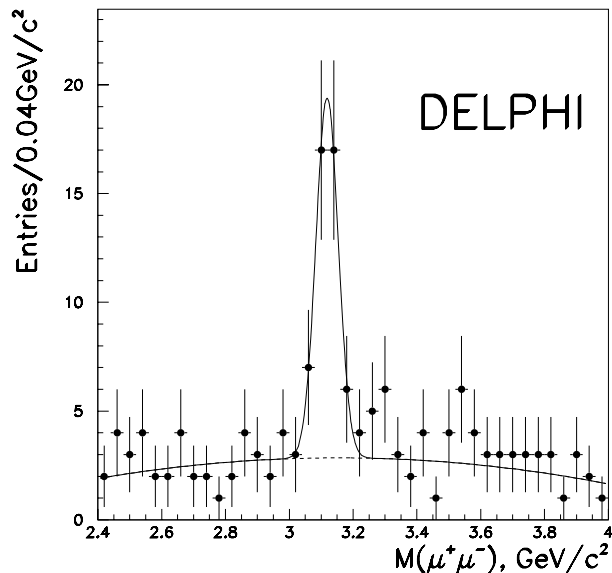


Figure 3: $M(\mu^+\mu^-)$ distribution from the LEP II DELPHI data. The solid curve corresponds to a Gaussian fit over a second order polynomial background.

The observed width of the peak is consistent within errors with the invariant mass resolution of a pair of charged particle tracks in the mass region around $3 \text{ GeV}/c^2$. The number of observed events from the fit is:

$$N(J/\psi) = 36 \pm 7 \text{ events},$$

over a background of about 11 events.

If we take the L3 result [6] for the beauty cross-section from $\gamma\gamma$ events and the PDG value [7] for the branching ratio of beauty hadrons to J/ψ , the expected number of $J/\psi \rightarrow \mu^+\mu^-$ from beauty hadrons is 2.1 ± 0.6 . The backgrounds from the processes $e^+ + e^- \rightarrow Z + \gamma \rightarrow J/\psi + X$ and $\gamma + \gamma \rightarrow \chi_{c2} \rightarrow J/\psi + \pi^+ + \pi^- + \pi^0$ are less than 0.20 and 0.30 event respectively. According to the selection criteria the system X contains at least two charged particle tracks, hence we do not consider such sources of J/ψ production as $\gamma + \gamma \rightarrow \chi_{c2} \rightarrow J/\psi + \gamma$. We checked that in the four-prong events with $J/\psi \rightarrow \mu^+\mu^-$ candidates there are no photon conversions.

We used the PYTHIA 6.156 generator [8] to estimate the efficiency. The generated events were passed through the simulation package of the DELPHI detector [5] and then processed with the same reconstruction and analysis programs as the real data. There is a substantial fraction of PYTHIA events where J/ψ mesons are produced just as a simple fusion of two photons because there is not enough phase space to produce additional particles. We do not use such events. The process where both photons are VDM photons we will call ‘diffractive’ and the process without VDM photons we will call ‘resolved’.

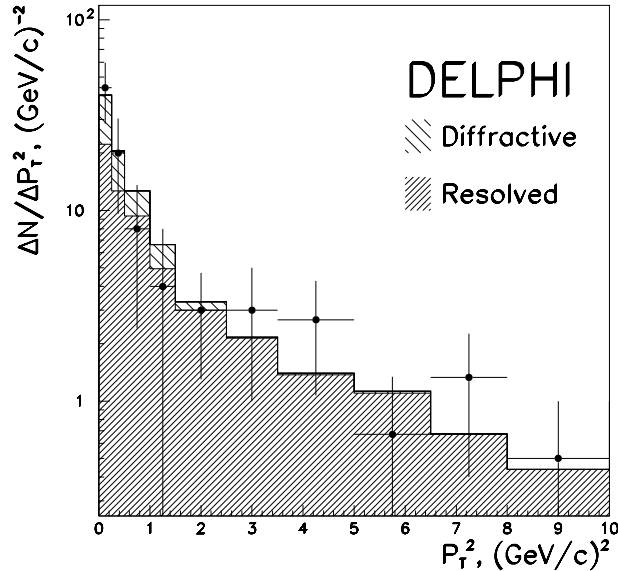


Figure 4: $p_T^2(J/\psi)$ distribution from the LEP II DELPHI data, shown as points with error bars. The histogram is a combination of the normalized ‘resolved’ and ‘diffractive’ processes from PYTHIA (see text).

A set of the J/ψ production characteristics is exhibited in Figs.4 to 8. For each bin of every distribution shown, we have examined the $M(\mu^+\mu^-)$ spectrum and then fitted with a Gaussian and a second order polynomial background, to get the number of signal events per bin. This number is then renormalized for each distribution, so that the total sum is always equal to 36 events. Hence, Fig.4 to Fig.8 are background subtracted distributions.

Fig. 4 shows the $p_T^2(J/\psi)$ distribution. As expected, the PYTHIA Monte Carlo prediction for the $p_T^2(J/\psi)$ distribution is more sharply peaked near zero for the ‘diffractive’ events (see Fig. 1a) than for the ‘resolved’ events (see Fig. 1b). We fitted the experimental $p_T^2(J/\psi)$ distribution as a function of the two categories of PYTHIA events:

$$\frac{dN}{dp_T^2} = f \cdot \left. \frac{dN}{dp_T^2} \right|_{\text{Diffractive}} + (1 - f) \cdot \left. \frac{dN}{dp_T^2} \right|_{\text{Resolved}}, \quad (5)$$

which gives $f = (26 \pm 22)\%$ (PYTHIA distributions in Fig. 4 are normalized to the data). The PYTHIA study tells us that the experimental efficiencies are very different for the two categories:

$$\begin{aligned} \epsilon(\text{diffractive}) &= (0.98 \pm 0.04)\%, \\ \epsilon(\text{resolved}) &= (3.87 \pm 0.09)\%. \end{aligned} \quad (6)$$

According to PYTHIA, about one-half of all the $\gamma\gamma$ events with $J/\psi \rightarrow \mu^+\mu^-$ are produced with the charged particle tracks at polar angles below 10 degrees, so that they are invisible

to the DELPHI detector. The individual efficiencies as a function of p_T^2 are given in Fig. 5. Some insight may be gained into these efficiencies if they are broken down into products of two factors, as follows:

$$\begin{aligned}\epsilon(\text{diffractive}) &= \epsilon_{\gamma\gamma}(\text{diffractive}) \times \epsilon_{J/\psi \rightarrow \mu^+\mu^-}(\text{diffractive}), \\ \epsilon(\text{resolved}) &= \epsilon_{\gamma\gamma}(\text{resolved}) \times \epsilon_{J/\psi \rightarrow \mu^+\mu^-}(\text{resolved}),\end{aligned}\quad (7)$$

where $\epsilon_{\gamma\gamma}$ is the efficiency for the process $\gamma\gamma \rightarrow J/\psi + X$ and $\epsilon_{J/\psi \rightarrow \mu^+\mu^-}$ is that for $J/\psi \rightarrow \mu^+\mu^-$. As expected, the latter is relatively process-independent:

$$\begin{aligned}\epsilon_{J/\psi \rightarrow \mu^+\mu^-}(\text{diffractive}) &= (37.0 \pm 1.5)\%, \\ \epsilon_{J/\psi \rightarrow \mu^+\mu^-}(\text{resolved}) &= (32.1 \pm 0.7)\%.\end{aligned}\quad (8)$$

It is clear, therefore, that the difference in efficiency in (6) is mostly due to $\epsilon_{\gamma\gamma}$. This is highly process-dependent and hence model-dependent.

The overall experimental efficiency is:

$$\frac{1}{\epsilon} = \frac{f}{\epsilon(\text{diffractive})} + \frac{1-f}{\epsilon(\text{resolved})},\quad (9)$$

which gives $\epsilon = (2.19_{-0.59}^{+1.27})\%$. Under the assumption that PYTHIA captures the kinematical features of the resolved and diffractive processes, but not their absolute cross-sections, the cross-section for inclusive J/ψ production is:

$$\sigma = N(J/\psi) \cdot (Br \cdot \mathcal{L} \cdot \epsilon)^{-1} = 45 \pm 9(\text{stat}) \pm 17(\text{syst}) \text{ pb},\quad (10)$$

where $Br = (5.88 \pm 0.10)\%$ is the branching ratio for $J/\psi \rightarrow \mu^+\mu^-$ [7] and $\mathcal{L} = 617 \text{ pb}^{-1}$ is the total integrated luminosity. The systematic uncertainties include both the efficiency (9) and the branching ratio contributions but not those inherent to the PYTHIA program.

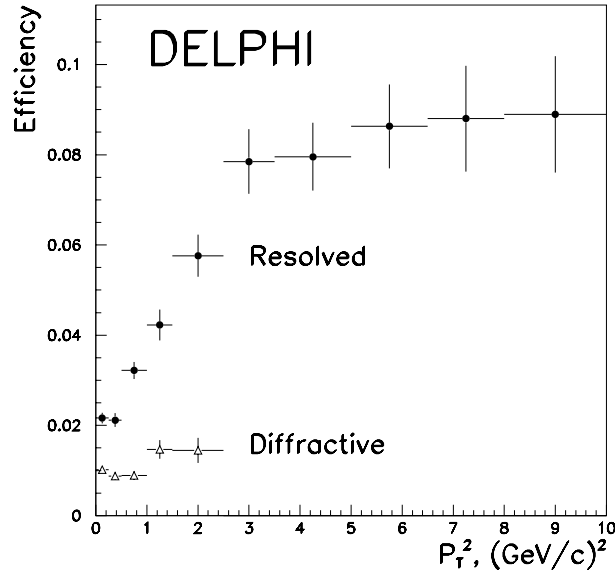


Figure 5: Efficiencies for resolved and diffractive processes as functions of p_T^2 .

Because of the model-dependent aspect of this analysis (see, for example, the efficiencies given in (6)), it is of interest to quote the ‘visible’ cross-section. Substituting

$\epsilon_{J/\psi \rightarrow \mu^+ \mu^-}$ (diffractive) and $\epsilon_{J/\psi \rightarrow \mu^+ \mu^-}$ (resolved) for ϵ (diffractive) and ϵ (resolved) respectively in (9), the ‘visible’ cross-section can be calculated; it is:

$$\sigma_{\text{vis}} = 3.0 \pm 0.6(\text{stat}) \pm 0.1(\text{syst}) \text{ pb.} \quad (11)$$

The main source of systematic uncertainty comes from the determination of the relative fractions of resolved and diffractive events which have different efficiencies (8). Following the same argument, we also give the ‘visible’ production rate $\langle n \rangle$ for J/ψ production:

$$\langle n \rangle = N(J/\psi) \cdot \left(N_t \cdot Br \cdot \epsilon_{J/\psi \rightarrow \mu^+ \mu^-} \right)^{-1} = (6.7 \pm 1.3(\text{stat}) \pm 0.3(\text{syst})) \times 10^{-3}, \quad (12)$$

where N_t is the data sample for the $\gamma\gamma$ selection as given in the previous section.

The rapidity distribution in the laboratory system for the J/ψ mesons is shown in Fig. 6. The PYTHIA events have been combined using the same fraction f found in (5) and then normalized to the observed number of events in $0 < |y| < 2.0$. The same techniques have been used to compare the experimental distributions of $M(J/\psi + X)$, $M(X)$, the charged and total multiplicities [$N_{\text{ch}}(X)$ and $N_{\text{tot}}(X)$], in Figs. 7a–d. There is fair agreement within statistics between the shapes of our measured distributions and the PYTHIA predictions (using the best fit as found in (5) for the relative content of diffractive and resolved events and renormalizing the PYTHIA prediction to the number of observed events).

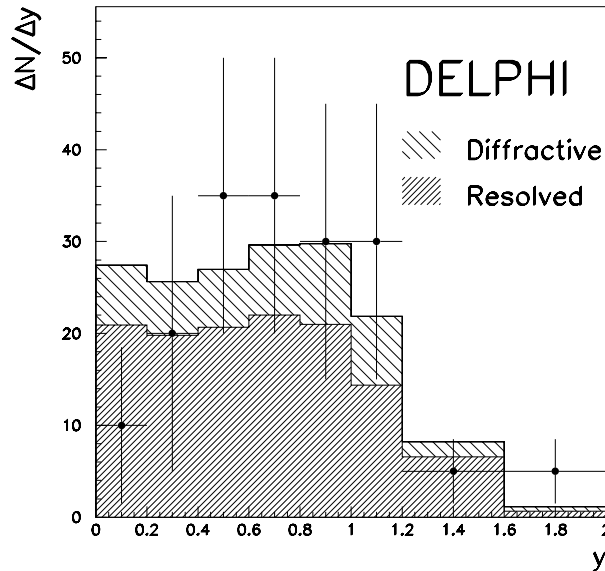


Figure 6: $|y|$ distribution for J/ψ mesons from the LEP II DELPHI data, shown as points with error bars. The histogram is a combination of the normalized ‘resolved’ and ‘diffractive’ processes from PYTHIA (see text).

The acceptance-corrected distributions in $\cos \theta$, where θ is the helicity angle of μ^+ in the rest frame of $J/\psi \rightarrow \mu^+ \mu^-$, are shown in Figs. 8a–c, along with the results of a fit to the form $(1 + a \cos^2 \theta)$. The fitted parameters are $a = -0.9 \pm 0.6$ for the total sample (a), $a = -1.8 \pm 0.5$ for $p_T^2(J/\psi) < 1.0$ (GeV/c^2) (b) and $a = 0.7 \pm 1.3$ for $p_T^2(J/\psi) > 1.0$ (GeV/c^2) (c). These results indicate that the J/ψ mesons are produced with little polarization at high $p_T^2(J/\psi)$, where the main contribution comes from the resolved processes.

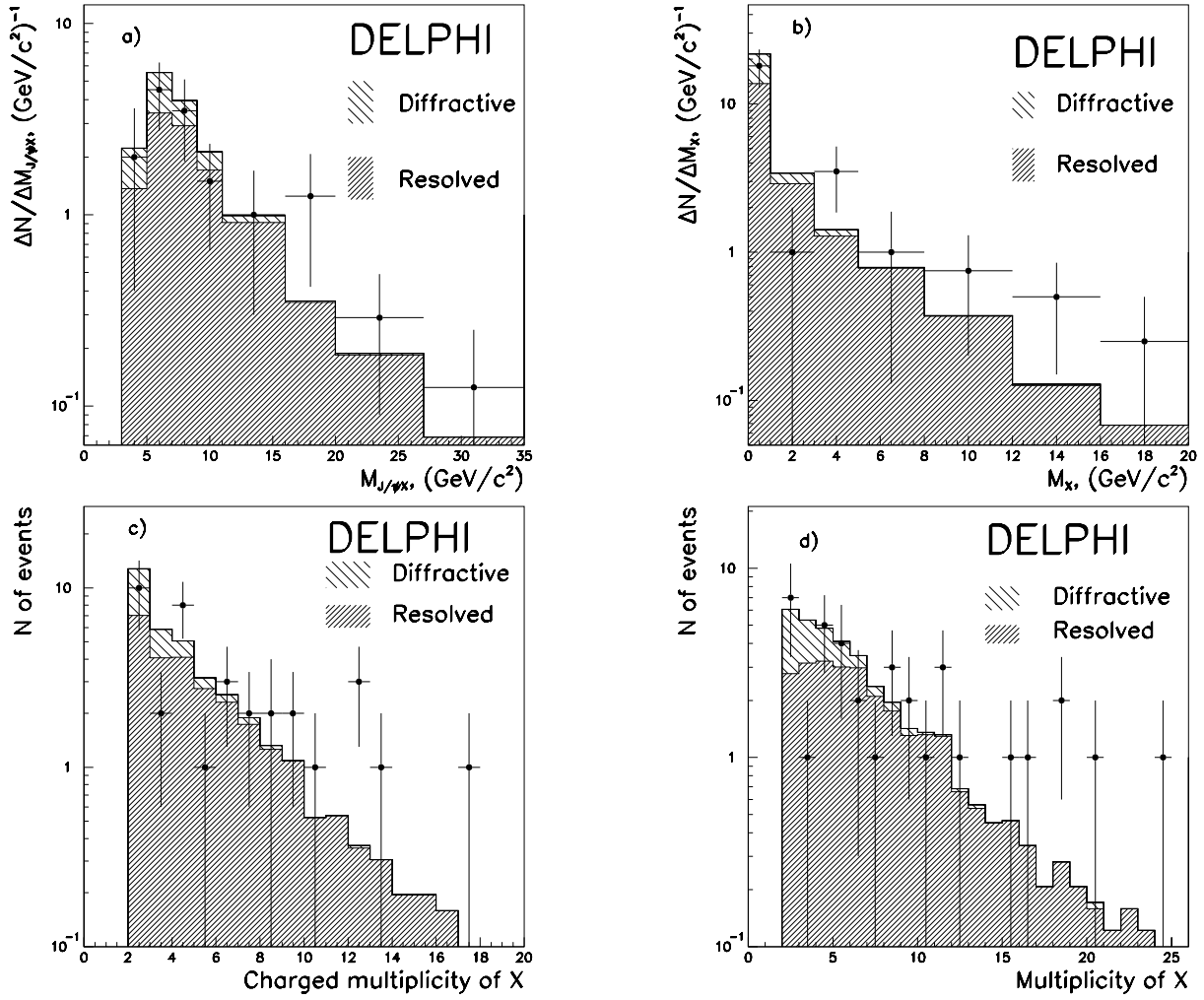


Figure 7: Visible distributions of $M(J/\psi + X)$ (a), $M(X)$ (b), charged (c) and total (d) multiplicities of the X system. Each histogram is a combination of the normalized 'resolved' and 'diffractive' processes from PYTHIA (see text).

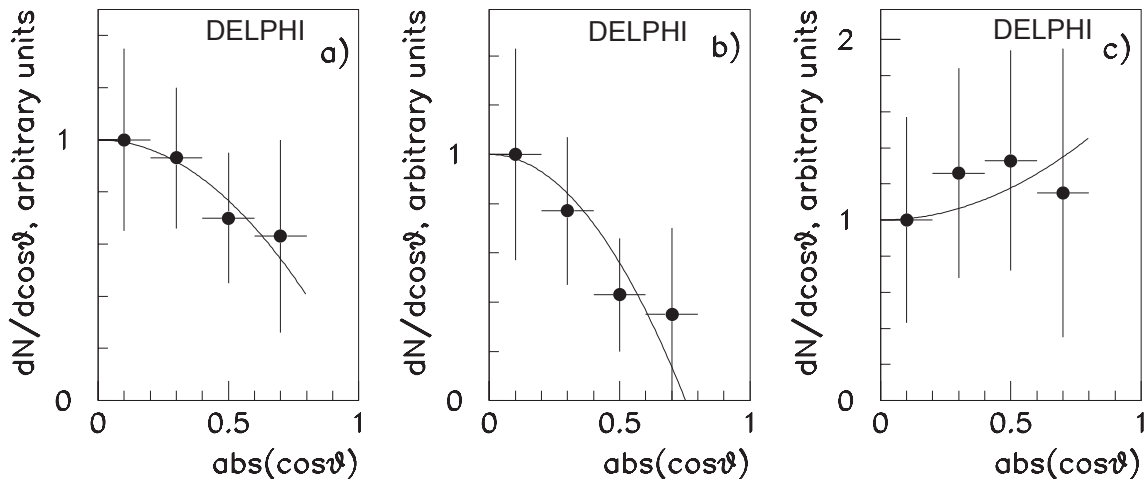


Figure 8: Acceptance-corrected distributions in $\cos\theta$ where θ is the helicity angle of μ^+ in the rest frame of $J/\psi \rightarrow \mu^+\mu^-$. The figures (a-c) correspond to the total sample (a), the subsamples with $p_T^2(J/\psi) < 1.0 (\text{GeV}/c)^2$ (b) and $p_T^2(J/\psi) > 1.0 (\text{GeV}/c)^2$ (c).

4 Conclusions

We have studied the inclusive J/ψ production from $\gamma\gamma$ collisions. The data have been taken by the DELPHI Collaboration during the LEP II phase, i.e. \sqrt{s} of the LEP machine ranged from 161 to 207 GeV. A clear signal from the reaction $\gamma\gamma \rightarrow J/\psi + X$ is seen.

The inclusive cross-section is estimated to be $\sigma(J/\psi + X) = 45 \pm 9(\text{stat}) \pm 17(\text{syst})$ pb. Based on a study of the p_T^2 distribution of different types of $\gamma\gamma$ processes in the PYTHIA program, we conclude that some $(74 \pm 22)\%$ of the observed J/ψ events are due to the ‘resolved’ photons, the dominant contribution of which should correspond to the gluon content of the photon [3].

The distributions in $p_T^2(J/\psi)$, y and $\cos\theta$ (for μ^+ in the rest frame of $J/\psi \rightarrow \mu^+\mu^-$) are presented. In addition, a study is given of the characteristics of the system X . All distributions appear to be well reproduced within statistics by the normalized combination of the fitted ‘resolved’ and ‘diffractive’ contributions.

Acknowledgements

We are greatly indebted to our technical collaborators, to the members of the CERN-SL Division for the excellent performance of the LEP collider, and to the funding agencies for their support in building and operating the DELPHI detector.

We acknowledge in particular the support of

Austrian Federal Ministry of Education, Science and Culture, GZ 616.364/2-III/2a/98,
FNRS-FWO, Flanders Institute to encourage scientific and technological research in the industry (IWT), Federal Office for Scientific, Technical and Cultural affairs (OSTC), Belgium,

FINEP, CNPq, CAPES, FUJB and FAPERJ, Brazil,

Czech Ministry of Industry and Trade, GA CR 202/99/1362,

Commission of the European Communities (DG XII),

Direction des Sciences de la Matière, CEA, France,

Bundesministerium für Bildung, Wissenschaft, Forschung und Technologie, Germany,

General Secretariat for Research and Technology, Greece,

National Science Foundation (NSF) and Foundation for Research on Matter (FOM),

The Netherlands,

Norwegian Research Council,

State Committee for Scientific Research, Poland, SPUB-M/CERN/PO3/DZ296/2000,

SPUB-M/CERN/PO3/DZ297/2000 and 2P03B 104 19 and 2P03B 69 23(2002-2004)

JNICT-Junta Nacional de Investigação Científica e Tecnológica, Portugal,

Vedecka grantova agentura MS SR, Slovakia, Nr. 95/5195/134,

Ministry of Science and Technology of the Republic of Slovenia,

CICYT, Spain, AEN99-0950 and AEN99-0761,

The Swedish Natural Science Research Council,

Particle Physics and Astronomy Research Council, UK,

Department of Energy, USA, DE-FG02-01ER41155,

EEC RTN contract HPRN-CT-00292-2002.

We are indebted to Dr. T. Sjöstrand for his help with the diagrams included in this paper and for his comments on PYTHIA. We thank M. Klasen for his help with the diagrams important for inclusive J/ψ production. S.-U. Chung is grateful for the warm hospitality extended to him by the CERN staff during his sabbatical year in the EP Division.

References

- [1] ‘Physics at LEP2,’ edited by G. Altarelli, T. Sjöstrand and F. Zwirner, CERN96-01 (Vol. 1), Feb 1996.
See Section 7 (heavy-quark physics), p. 330, in the chapter on $\gamma\gamma$ physics.
- [2] J.J. Sakurai and D. Schildknecht, Phys. Lett. **B40** (1979) 121;
I. F. Ginzburg and V.G. Serbo, Phys. Lett. **B109** (1982) 231.
- [3] R. M. Godbole *et al.*, Phys. Rev. **D65** (2002) 074003;
M. Klasen *et al.*, Nucl. Phys. **B609** (2001) 518;
B. Naroska, Nucl. Phys. B (Proc. Suppl.) **82** (2000) 187;
H. Jung, G. A. Schuler and J. Terrón, Int. J. Mod. Phys. **A7** (1992) 7955;
E. L. Berger and D. Jones, Phys. Rev. **D23** (1981) 1521.
- [4] P. Aarnio *et al.*, DELPHI Collab., Nucl. Inst. Meth. **A303** (1991) 233.
- [5] P. Abreu *et al.*, DELPHI Collab., Nucl. Inst. Meth. **A378** (1996) 57.
- [6] R. Acciarri *et al.*, L3 Collab., Phys. Lett. **B503** (2001) 10.
- [7] Particle Data Group, K.Hagiwara *et al.*, Phys. Rev. **D66**, 010001 (2002).
- [8] T. Sjöstrand *et al.*, Comput. Phys. Comm. **135** (2001) 238.